

## Supporting Information

### **Ensembles of Cationic Conjugated Polymer and Anionic Platinum(II) Complexes: From FRET Properties to Application Studies in *E. coli* Imaging and Singlet Oxygen Generation**

Angela Lok-Yin So,<sup>#a</sup> Jungu Guo,<sup>#a</sup> Huanxiang Yuan,<sup>b</sup> Qi Shen,<sup>b</sup> Eric Ka-Ho Wong,<sup>a</sup> Shu Wang<sup>\*b</sup> and Vivian Wing-Wah Yam<sup>\*a</sup>

<sup>a</sup>Institute of Molecular Functional Materials and Department of Chemistry, The University of Hong Kong, Pokfulam Road, Hong Kong, PR China.

<sup>b</sup>Beijing National Laboratory for Molecular Sciences, Key Laboratory of Organic Solids, Institute of Chemistry, Chinese Academy of Sciences, Beijing, PR China.

E-mail: wwyam@hku.hk; wangshu@iccas.ac.cn

## Physical Measurements and Instrumentation

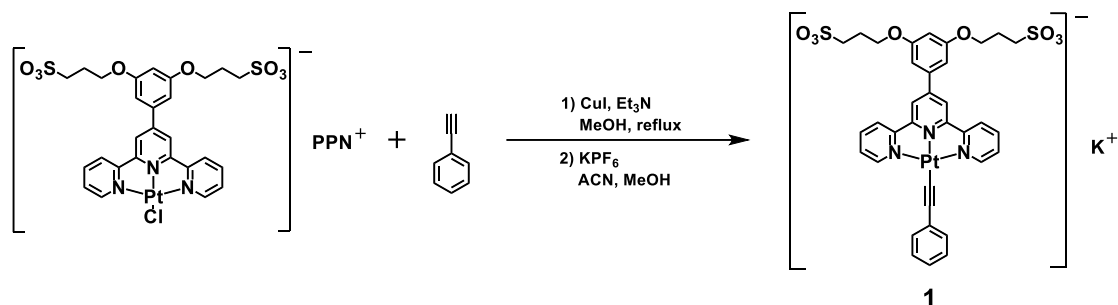
The  $^1\text{H}$  and  $^{13}\text{C}\{^1\text{H}\}$  NMR spectra were recorded on a Bruker AVANCE 400 (400 MHz), a Bruker Ascend 500 (500 MHz) or a Bruker AVANCE 600 (600 MHz) Fourier Transform NMR Spectrometer with chemical shifts relative to tetramethylsilane ( $\text{Me}_4\text{Si}$ ).  $^1\text{H}$  NMR spectra were recorded in  $\text{DMSO-}d_6$  since broad and featureless  $^1\text{H}$  NMR signals were observed for samples in  $\text{D}_2\text{O}$  (Figure S23), possibly due to the formation of aggregates. The positive-ion and negative-ion electrospray ionization (ESI) mass spectra were recorded on a Bruker maXis II high-resolution ESI-QTOF mass spectrometer. Elemental analysis was carried out on a Thermo Scientific Flash EA 1112 Elemental Analyzer at the Institute of Chemistry, Chinese Academy of Sciences. UV-Vis absorption spectra were collected on an Agilent Cary 60 UV-Vis Spectrophotometer with a xenon flash lamp. Steady-state emission spectra were recorded on an Edinburgh Instruments FS5 fluorescence spectrophotometer equipped with an R928P PMT detector. The determination of microbial concentration was measured on a JASCO V-550 spectrophotometer. Confocal microscopy experiments were performed with a confocal laser scanning microscope (FV1200-IX81, Olympus, Japan). Relative luminescence quantum yields of  $\text{PFP-NMe}_3^+$  in aqueous solution at 298 K were measured by optical dilution method by Demas and Crosby<sup>1</sup> using quinine sulfate in 1.0 N  $\text{H}_2\text{SO}_4$  (excitation wavelength = 365 nm,  $\Phi = 0.546$ ) as the reference.<sup>2</sup> White light irradiation was provided by Simulated Sunlight, Beijing education Au-light technology (CEL-PE300L). Excited-state lifetimes of solution samples were measured on a Hamamatsu C11367-34 Quantaurus-Tau

Fluorescence lifetime spectrometer.

## Material and Reagents

Potassium tetrachloroplatinate(II) ( $K_2[PtCl_4]$ ) (Chem. Pur., 98 %), triethylamine (Thermo Fisher), copper(I) iodide (AK Scientific, 98%), trimethylsilylacetylene (GFS chemicals), phenylacetylene (AK Scientific, 98%), 4-iodophenol (AK Scientific, 98%) and (4-bromophenyl)benzothiazole (Sigma-Aldrich) were purchased from the corresponding company. Other chemicals were purchased from Arcos, Alfa-Aesar, AK Scientific, and Sigma-Aldrich. The Amp<sup>r</sup> *Escherichia coli* (*E. coli*) was purchased from Beijing Bio-Med Technology Development Co., Ltd. Poly(fluorene-co-phenylene) derivative (PFP-NMe<sub>3</sub><sup>+</sup>),<sup>3</sup>  $[Pt\{tpy-C_6H_3-(OPrSO_3)_2\}Cl]PPN$ ,<sup>4</sup>  $[Pt\{bzimpy(PrSO_3)_2\}Cl]PPN$ ,<sup>5</sup>  $[Pt\{tpy-(C_6H_4CH_2NMe_3-4)-4'\}Cl]PF_6$ ,<sup>6</sup>  $H-C\equiv C-C_6H_4-OC_{12}H_{25}$ ,<sup>7</sup>  $H-C\equiv C-C_6H_4$ -benzothiazole<sup>8</sup> and  $[Pt\{bzimpy(PrSO_3)_2\}\{C\equiv C-C_6H_4-OC_{12}H_{25}\}]K$  (**2**)<sup>9</sup> were prepared according to literature procedures. All other reagents and solvents were of analytical grade and were used without any treatment. Deionized water used was purified with Elga Purelab UHQ system. All reactions were performed under inert conditions using standard Schlenk techniques unless specified otherwise.

## Synthesis and Experimental Procedures



**Scheme S1.** Synthetic route for complex 1.

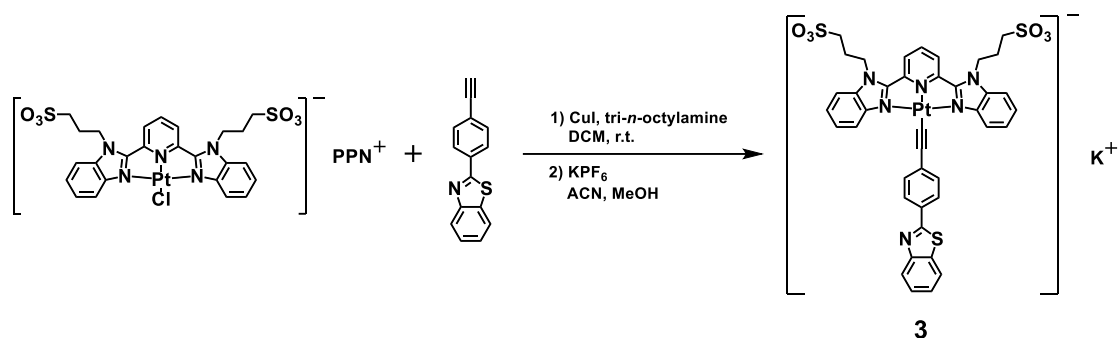
### Synthesis of $[Pt\{tpy-C_6H_3-(OPrSO_3)_2\}\{C\equiv C-C_6H_5\}]K$ (1)

This was synthesized according to the modification of procedures from previous literature.<sup>4</sup> To a solution of  $[Pt\{tpy-C_6H_3-(OPrSO_3)_2\}Cl]PPN$  (0.20 g, 0.07 mmol) in degassed methanol (50 mL) was added phenylacetylene (0.02 mL, 0.22 mmol) in the presence of triethylamine (2 mL) and a catalytic amount of  $CuI$ . The mixture was heated under reflux overnight under inert atmosphere. After removal of solvents, the residue was washed with diethyl ether. Recrystallization was carried out by slow diffusion of diethyl ether vapor into a concentrated methanol solution to afford the pure product in  $PPN^+$  salt as a red solid. The product was converted to  $K^+$  salt by salt metathesis reaction by reacting with  $KPF_6$  in acetonitrile–methanol mixture, and the precipitates were collected by filtration. The product was purified by washing with acetonitrile to afford a yellow solid. Yield: 0.09 g (48 %).  $^1H$  NMR (400 MHz,  $DMSO-d_6$ , 298 K,  $\delta/ppm$ )  $\delta$  2.10 (m, 4H,  $-CH_2-$ ), 2.66 (m, 4H,  $-CH_2SO_3$ ), 4.29 (m, 4H,  $-OCH_2-$ ), 6.66 (s, 1H, phenyl), 7.21–7.23 (m, 1H, phenyl), 7.24–7.28 (m, 2H, phenyl),

7.36–7.38 (m, 4H, phenyl), 7.78 (m, 2H, terpyridine), 8.29–8.33 (t,  $J = 8.0$  Hz, 2H, terpyridine), 8.87–8.90 (m, 4H, terpyridine), 8.95–8.97 (m, 2H, terpyridine).  $^{13}\text{C}\{^1\text{H}\}$  NMR (600 MHz, DMSO- $d_6$ , 298 K,  $\delta$  /ppm) 160.27, 158.43, 153.68, 153.58, 152.17, 141.56, 136.37, 131.57, 129.40, 127.93, 126.43, 126.33, 126.18, 121.11, 105.91, 104.10, 103.26, 98.80, 66.67, 47.44, 24.71. HRMS (negative-ion ESI): calcd.  $\text{C}_{35}\text{H}_{30}\text{N}_3\text{O}_8\text{PtS}_2$   $m/z = 879.1119$ ; found: 879.1091  $[\text{M}-\text{K}]^-$ .

### Synthesis of $[\text{Pt}\{\text{bzimpy}(\text{PrSO}_3)_2\}\{\text{C}\equiv\text{C}-\text{C}_6\text{H}_4-\text{OC}_{12}\text{H}_{25}\}]\text{K}$ (**2**)

This was synthesized according to the procedures from previous literature.<sup>9</sup>  $^1\text{H}$  NMR (400 MHz, DMSO- $d_6$ , 298 K,  $\delta$  /ppm):  $\delta$  0.86 (t,  $J = 6.8$  Hz, 3H,  $-\text{CH}_3$ ), 1.26–1.45 (m, 18H,  $-\text{CH}_2-$ ), 1.73–1.79 (m, 2H,  $-\text{CH}_2-$ ), 2.20–2.22 (m, 4H,  $-\text{CH}_2-$ ), 2.67 (t,  $J = 6.4$  Hz, 4H,  $-\text{CH}_2\text{SO}_3$ ), 4.02 (t,  $J = 6.8$  Hz, 2H,  $-\text{OCH}_2-$ ), 5.00 (t,  $J = 6.4$  Hz, 4H,  $-\text{NCH}_2-$ ), 7.01 (d,  $J = 8.4$  Hz, 2H, phenyl), 7.41 (d,  $J = 8.4$  Hz, 2H, phenyl), 7.58–7.60 (m, 4H, benzimidazolyl), 8.00–8.02 (m, 2H, benzimidazolyl), 8.33 (t,  $J = 8.0$  Hz, 1H, pyridine), 8.54–8.56 (m, 2H, benzimidazolyl), 8.84 (d,  $J = 8.0$  Hz, 2H, pyridine).  $^{13}\text{C}\{^1\text{H}\}$  NMR (600 MHz, DMSO- $d_6$ , 298 K,  $\delta$  /ppm):  $\delta$  157.31, 153.79, 146.72, 142.58, 139.04, 134.21, 132.28, 126.33, 126.10, 124.82, 118.86, 117.67, 114.66, 112.83, 108.08, 88.15, 67.40, 47.40, 44.27, 31.20, 28.95, 28.92, 18.69, 28.62, 26.00, 25.44, 22.00, 13.86. HRMS (negative-ion ESI) calcd. for  $\text{C}_{45}\text{H}_{52}\text{N}_5\text{O}_7\text{PtS}_2$   $m/z = 1033.2964$ ; found  $m/z = 1033.2926$   $[\text{M}-\text{K}]^-$ . Elemental analysis calcd. (%) for  $\text{C}_{45}\text{H}_{52}\text{KN}_5\text{O}_7\text{PtS}_2 \cdot \text{H}_2\text{O}$ : C, 49.53; H, 4.99; N, 6.42; found: C, 49.40; H, 5.03; N, 6.03.

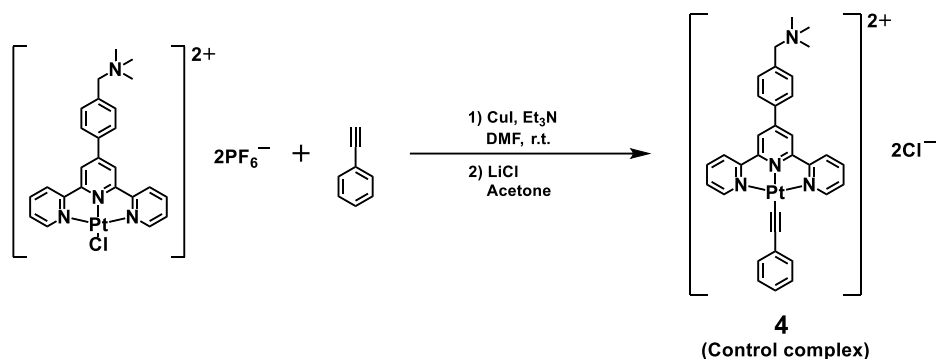


**Scheme S2.** Synthetic route for complex **3**.

### Synthesis of [Pt{bzimpy(PrSO<sub>3</sub>)<sub>2</sub>}{C≡C–C<sub>6</sub>H<sub>4</sub>–benzothiazole}]K (**3**)

The procedure was similar to that of **1**, by reacting [Pt{bzimpy(PrSO<sub>3</sub>)<sub>2</sub>}Cl]PPN (0.10 g, 0.08 mmol) in degassed dichloromethane (50 mL) with H–C≡C–C<sub>6</sub>H<sub>4</sub>–benzothiazole (0.07 g, 0.23 mmol) in the presence of tri-*n*-octylamine (5 mL) and a catalytic amount of CuI. The product was isolated as an orange solid. Yield: 0.03 g (35 %). <sup>1</sup>H NMR (400 MHz, DMSO-*d*<sub>6</sub>, 298 K,  $\delta$ /ppm):  $\delta$  2.18–2.20 (m, 4H, –CH<sub>2</sub>–), 2.67 (t, *J* = 6.4 Hz, 4H, –CH<sub>2</sub>SO<sub>3</sub>), 4.95 (t, *J* = 6.4 Hz, 4H, –NCH<sub>2</sub>–), 7.49 (t, *J* = 6.4 Hz, 1H, benzothiazolyl), 7.56–7.67 (m, 7H, benzimidazolyl, benzothiazolyl and phenyl), 7.94 (d, *J* = 6.4 Hz, 2H, benzimidazolyl), 8.12 (d, *J* = 6.4 Hz, 1H, benzothiazolyl), 8.18–8.22 (m, 3H, benzothiazolyl and phenyl), 8.30 (t, *J* = 6.8 Hz, 1H, pyridine), 8.42 (d, *J* = 6.4 Hz, 2H, benzimidazolyl), 8.87 (d, *J* = 6.8 Hz, 2H, pyridine). <sup>13</sup>C{<sup>1</sup>H} NMR (600 MHz, DMSO-*d*<sub>6</sub>, 298 K,  $\delta$ /ppm):  $\delta$  25.99, 44.31, 47.37, 88.76, 107.99, 112.84, 122.27, 124.86, 125.39, 126.16, 126.58, 127.50, 129.49, 130.47, 132.00, 134.03, 134.42, 138.86, 143.03, 146.72, 153.58, 166.87. HRMS (negative-ion ESI) calcd. for C<sub>40</sub>H<sub>31</sub>N<sub>6</sub>O<sub>6</sub>PtS<sub>3</sub> *m/z* = 982.1167; found *m/z* = 982.1081 [M–K]<sup>–</sup>. Elemental analysis calcd. (%) for C<sub>40</sub>H<sub>31</sub>KN<sub>6</sub>O<sub>6</sub>PtS<sub>3</sub>·3H<sub>2</sub>O: C, 44.65; H, 3.47; N,

7.81; found: C, 44.11; H, 3.41; N, 7.38.



**Scheme S3.** Synthetic route for the control complex **4**.

### Synthesis of [Pt{tpy-(C<sub>6</sub>H<sub>4</sub>CH<sub>2</sub>NMe<sub>3</sub>-4)-4'}ed{C≡C-C<sub>6</sub>H<sub>5</sub>}]Cl<sub>2</sub> (**4**)

The procedure was similar to that of **1**, by reacting [Pt{tpy-(C<sub>6</sub>H<sub>4</sub>CH<sub>2</sub>NMe<sub>3</sub>-4)-4'}Cl]PF<sub>6</sub> (0.10 g, 0.11 mmol) in degassed dimethylformamide (10 mL) with triethylamine (1 mL), phenylacetylene (0.04 mL, 0.33 mmol), and a catalytic amount of CuI. The product was converted to Cl<sup>-</sup> salt by salt metathesis reaction by reacting with LiCl in acetone, and the precipitates were collected by filtration. Subsequent recrystallization by diffusion of diethyl ether vapor into a concentrated methanol-acetonitrile solution of the crude product, followed by successive washing with dichloromethane and diethyl ether afforded the final product as a dark-red solid. Yield: 0.04 g (46 %). <sup>1</sup>H NMR (400 MHz, DMSO-*d*<sub>6</sub>, 298 K,  $\delta$ /ppm)  $\delta$  3.14 (s, 9H, -N(CH<sub>3</sub>)<sub>3</sub>), 4.74 (s, 2H, -CH<sub>2</sub>-), 7.25–7.28 (m, 1H, phenyl), 7.32–7.36 (t, *J* = 8.0 Hz, 2H, phenyl), 7.47–7.49 (d, *J* = 8.0 Hz, 2H, phenyl), 7.84–7.86 (d, *J* = 8.0 Hz, 2H, phenyl), 7.90–7.93 (t, *J* = 8.0 Hz, 2H, terpyridine), 8.38–8.40 (d, *J* = 8.0 Hz, 2H, phenyl), 8.51–8.55 (t, *J* = 8.0 Hz, 2H,

terpyridine), 8.96–8.98 (d,  $J = 8.0$  Hz, 2H, terpyridine), 9.10–9.11 (m, 2H, terpyridine), 9.17 (s, 2H, terpyridine).  $^{13}\text{C}\{^1\text{H}\}$  NMR (600 MHz, DMSO- $d_6$ , 298 K,  $\delta$ /ppm):  $\delta$  166.87, 153.58, 146.72, 143.03, 138.86, 134.42, 134.03, 132.00, 130.47, 129.49, 127.50, 126.58, 126.16, 125.39, 124.86, 122.77, 122.27, 117.25, 112.84, 107.99, 88.76, 47.37, 44.31, 25.99. HRMS (positive-ion ESI) calcd. for  $\text{C}_{33}\text{H}_{30}\text{N}_4\text{Pt}$   $m/z = 338.6055$ ; found:  $m/z = 338.6061$   $[\text{M}-2\text{Cl}]^{2+}$ . Elemental analysis calcd. (%) for  $\text{C}_{33}\text{H}_{30}\text{Cl}_2\text{N}_4\text{Pt}\cdot 1.5\text{CH}_2\text{Cl}_2\cdot\text{H}_2\text{O}$ : C, 46.35; H, 3.95; N, 6.27; found: C, 46.15; H, 4.05; N, 6.54.

### **Preparation of ensembles of PFP-NMe<sub>3</sub><sup>+</sup> and platinum(II) complexes**

Mixtures of PFP-NMe<sub>3</sub><sup>+</sup> and platinum(II) complexes were added in an aqueous solution and were mixed thoroughly. The final concentrations of PFP-NMe<sub>3</sub><sup>+</sup> and platinum(II) complex are 25  $\mu\text{M}$  and 50  $\mu\text{M}$  respectively to yield the same concentration of 50  $\mu\text{M}$  in both the anionic complexes and cationic trimethylammonium groups. The ensembles were used in pathogen imaging and determination of singlet oxygen ( $^1\text{O}_2$ ).

### **Confocal laser scanning microscopy (CLSM) characterization of microbes with various treatments**

Amp<sup>r</sup> *E. coli* were treated with PFP-NMe<sub>3</sub><sup>+</sup>, **3**, and the ensemble of PFP-NMe<sub>3</sub><sup>+</sup> and **3** at 37 °C for 30 minutes, these microbes (500  $\mu\text{L}$ , OD<sub>600</sub> = 1.0) were centrifuged (10000 rpm, 10 minutes) to remove the supernatant. The collected microbes were then washed with water for once and finally resuspended in 50

$\mu\text{L}$  of water for measurement. 5  $\mu\text{L}$  portion of the mixture was dropped on clean glass for imaging. The excitation wavelength is 405 nm and the emission wavelength ranges were collected from 425 nm to 525 nm with blue as pseudo color and 650 nm to 700 nm with red as pseudo color.

### Determination of singlet oxygen generation

2,2'-(Anthracene-9,10-diylbis(methylene))dimalonic acid (ABDA) was used as a specific probe for  $^1\text{O}_2$  in aqueous solution. An aqueous solution containing **1** or PFP- $\text{NMe}_3^+$  or the ensemble of PFP- $\text{NMe}_3^+$  and **1** in the presence of 100  $\mu\text{M}$  ABDA was irradiated with white light (20  $\text{mW cm}^{-2}$ ) for different periods of time. The  $^1\text{O}_2$  generation quantum yield ( $\Phi_\Delta$ ) could be determined by the following equation:<sup>10,11</sup>

$$\Phi_S = \Phi_R \times \frac{K_S}{K_R} \times \frac{A_R}{A_S}$$

where  $\Phi$  is the  $^1\text{O}_2$  generation quantum yield of the photosensitizer,  $K$  is the decomposition rate constants of ABDA which is determined as slopes of the plot of  $A/A_0$  against irradiation time,  $A$  is the light absorbed, and the subscript  $S$  and  $R$  refer to the sample and reference respectively.

Based on the above equation, a modified equation below could be used to determine the ratio of  $\Phi_\Delta$ :

$$\frac{\Phi_{ensemble}}{\Phi_{PFP}} = \frac{K_{ensemble}}{K_{PFP}} \times \frac{A_{PFP}}{A_{ensemble}}$$

where  $A$  is the light absorbed which is determined from the integration area of the absorption bands in the wavelength range of 300–600 nm, and the subscript

*ensemble* refers to the ensemble consisting of platinum(II) complex and PFP-NMe<sub>3</sub><sup>+</sup> while *PFP* refers to PFP-NMe<sub>3</sub><sup>+</sup>.

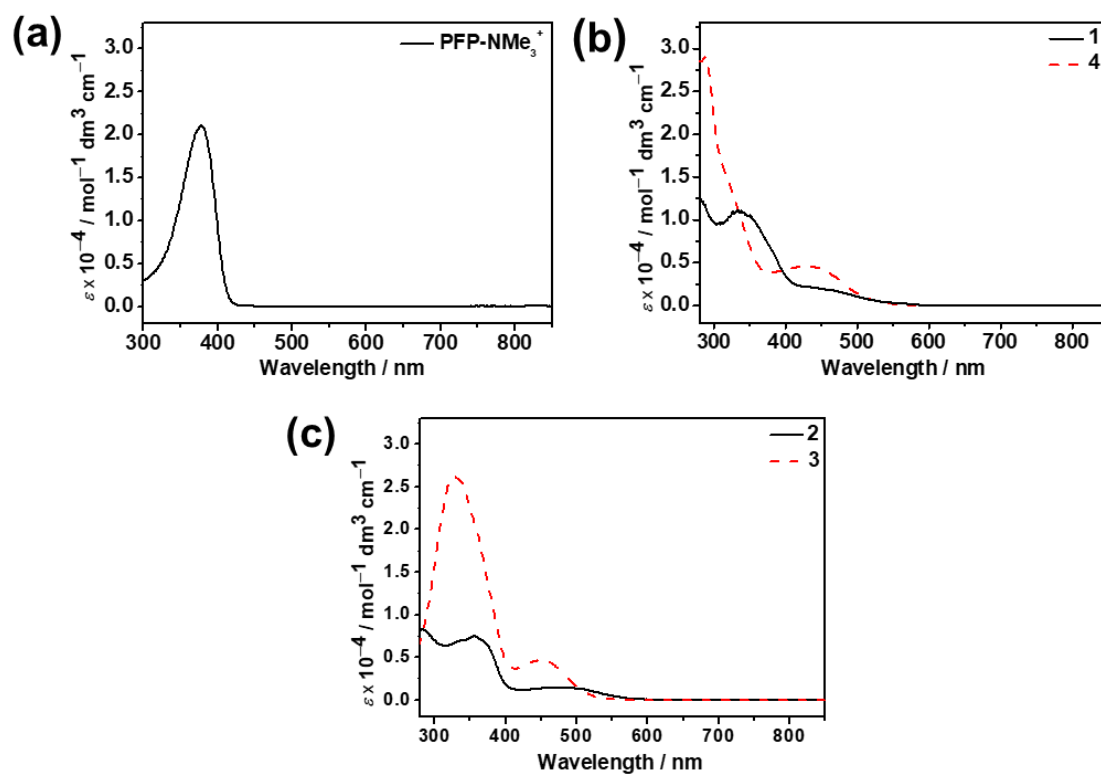


**Figure S1.** Electronic absorption spectra of (a) PFP-NMe<sub>3</sub><sup>+</sup> (50  $\mu\text{M}$ ) in water, (b) **1** (50  $\mu\text{M}$ ) and **4** (50  $\mu\text{M}$ ) in water, as well as (c) **2** (50  $\mu\text{M}$ ) and **3** (50  $\mu\text{M}$ ) in water-DMSO (19:1, v/v) mixture.

**Table S1.** Photophysical data of conjugated polymer PFP-NMe<sub>3</sub><sup>+</sup> and platinum(II) complexes **1–4** at 298 K

	Medium	$\lambda_{\text{abs}} / \text{nm}$ ( $\epsilon / \text{mol}^{-1} \text{dm}^3 \text{cm}^{-1}$ )
PFP-NMe <sub>3</sub> <sup>+</sup>	Water	375 (21290)
<b>1</b>	Water	334 (10860), 450 (1900)
<b>2</b>	Water–DMSO (19:1, v/v)	290 (7710), 355 (7370), 480 (1430)
<b>3</b>	Water–DMSO (19:1, v/v)	326 (26320), 450 (4580)
<b>4</b>	Water	288 (28790), 440 (4480)

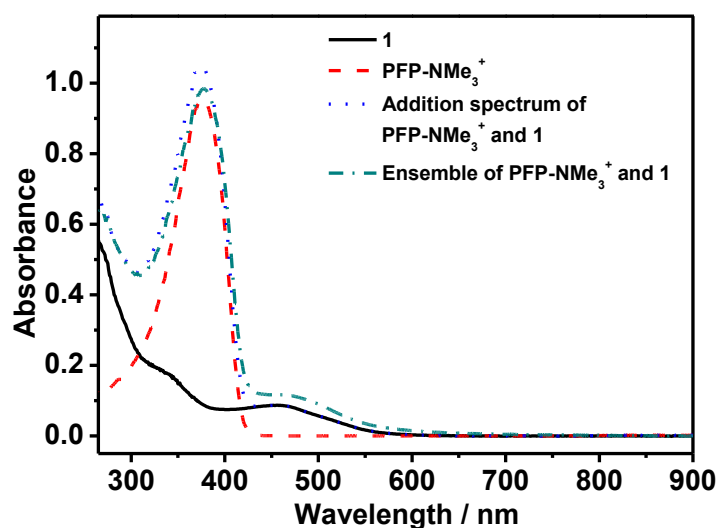


**Figure S2.** UV–Vis absorption spectra of **1** (50  $\mu\text{M}$ ), PFP-NMe<sub>3</sub><sup>+</sup> (50  $\mu\text{M}$ ), addition spectrum of PFP-NMe<sub>3</sub><sup>+</sup> (50  $\mu\text{M}$ ) **1** and (50  $\mu\text{M}$ ), as well as the ensemble of PFP-NMe<sub>3</sub><sup>+</sup> (50  $\mu\text{M}$ ) **1** and (50  $\mu\text{M}$ ) in water.

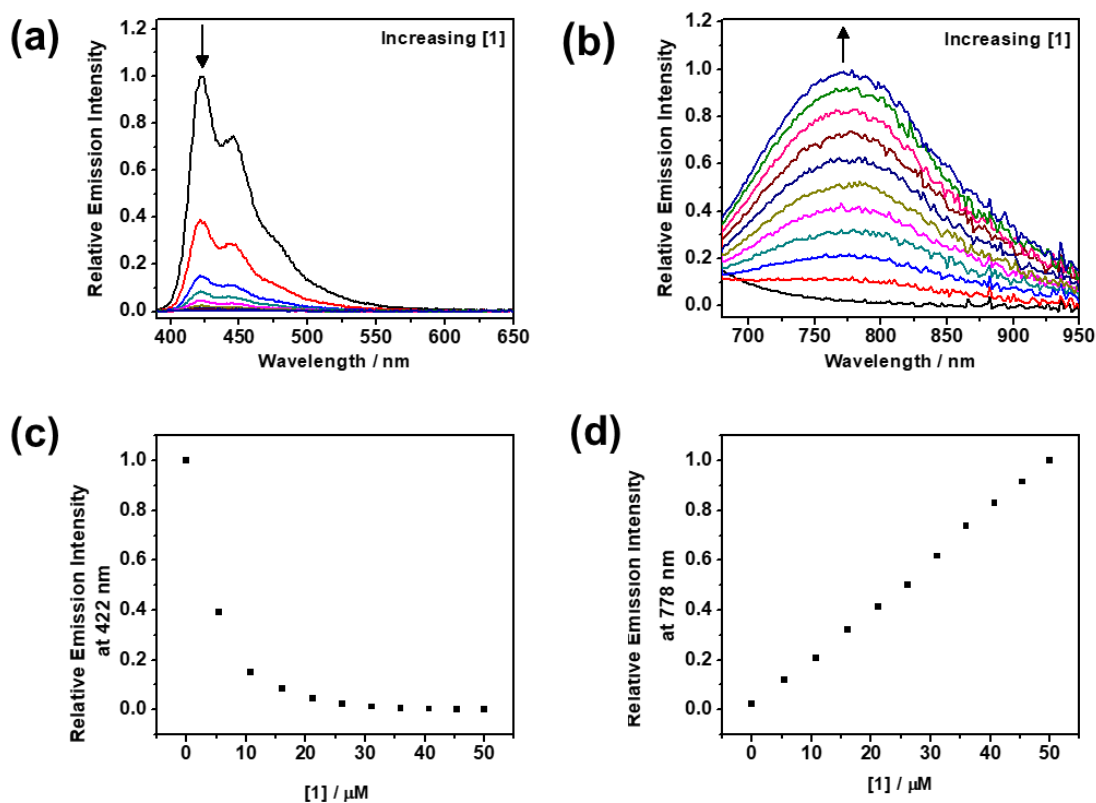


**Figure S3.** Emission spectral changes of PFP-NMe<sub>3</sub><sup>+</sup> (50 μM) in water upon addition of different concentrations of **1** (0–50 μM) in the range of (a) 390–650 nm and (b) 680–950 nm. (c) A plot of relative emission intensity at 422 nm against [1]. (d) A plot of relative emission intensity at 778 nm against [1]. An excitation wavelength of 355 nm was used.

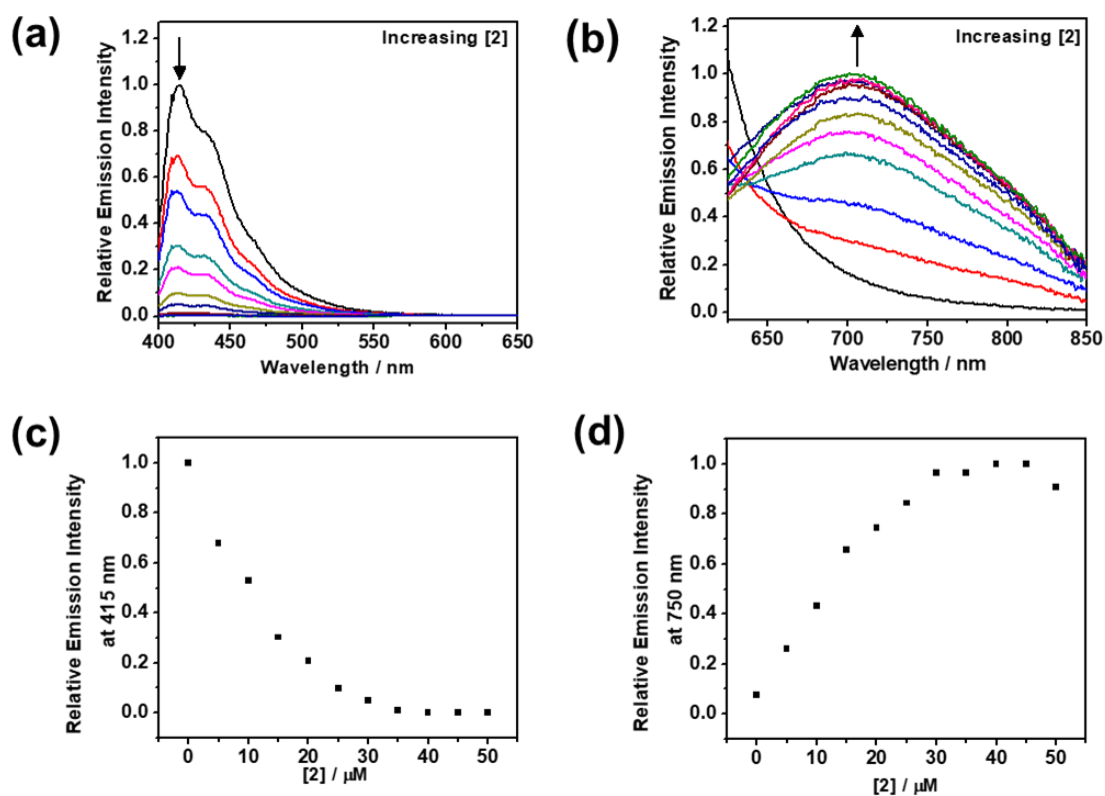


**Figure S4.** Emission spectral changes of PFP-NMe<sub>3</sub><sup>+</sup> (50 μM) in water–DMSO (19:1, v/v) mixture upon addition of different concentrations of **2** (0–50 μM) in the range of (a) 400–650 nm and (b) 600–850 nm. (c) A plot of relative emission intensity at 415 nm against [2]. (d) A plot of relative emission intensity at 750 nm against [2]. An excitation wavelength of 385 nm was used.

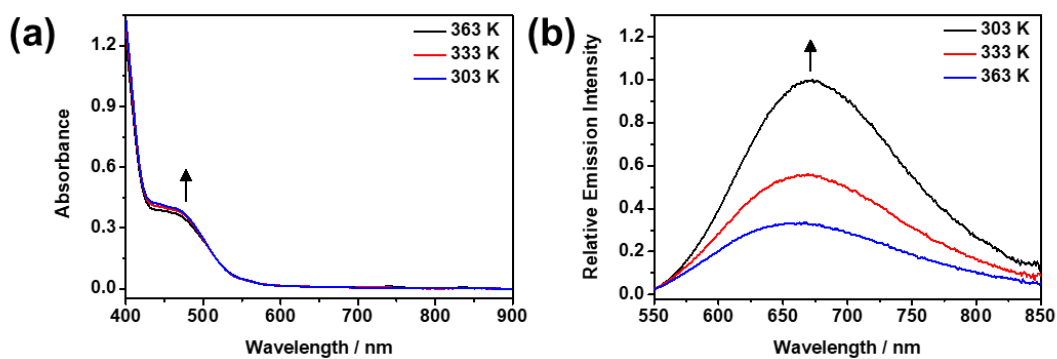


**Figure S5.** (a) UV-Vis absorption and (b) emission spectra of ensemble formed by PFP-NMe<sub>3</sub><sup>+</sup> (50 μM) and **3** (50 μM) in water-DMSO (19:1, v/v) mixture upon decreasing temperature from 363 to 303 K. An excitation wavelength of 385 nm was used in emission measurement.

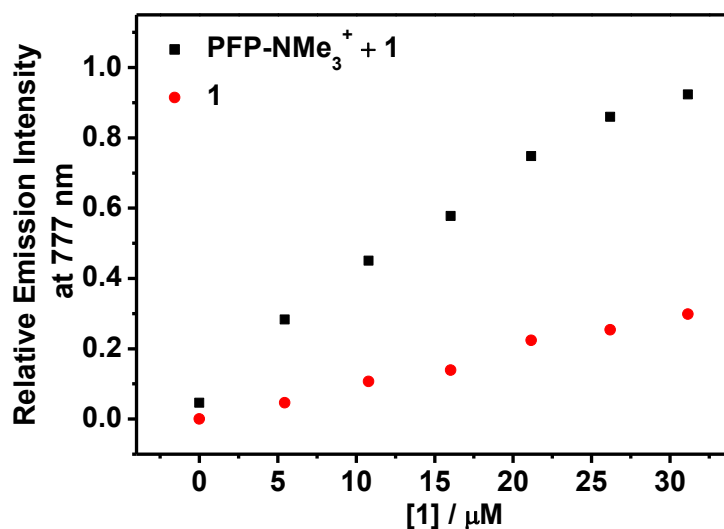


**Figure S6.** Plots of relative emission intensity at 777 nm against [1] in a solution of PFP-NMe<sub>3</sub><sup>+</sup> (50 μM) and **1** (0–50 μM) (black) as well as a solution of **1** (0–50 μM) (red) in water. An excitation wavelength of 355 nm was used.

**Table S2.** Stern–Volmer quenching constants ( $K_{sv}$ ) obtained from the emission spectra of PFP-NMe<sub>3</sub><sup>+</sup> in water with various concentrations of **1**

[1] / $\mu\text{M}$	$K_{sv} \times 10^{-5} / \text{M}^{-1}$
0	–
5.5	2.9
10.8	5.2
16.0	6.8
21.2	9.9
26.2	15.8
31.2	25.2
36.0	40.8
40.7	84.1
45.4	111.6
50.0	106.2

**Table S3.**  $K_{sv}$  obtained from the emission spectra of PFP-NMe<sub>3</sub><sup>+</sup> in water–DMSO (19:1, v/v) mixture with various concentrations of **2**

[2] / $\mu\text{M}$	$K_{sv} \times 10^{-5} / \text{M}^{-1}$
0	–
5.0	1.0
10.0	0.9
15.0	1.5
20.0	1.9
25.0	3.7
30.0	6.5
35.0	25.4
40.0	820.3
45.0	1535.2

**Table S4.**  $K_{SV}$  obtained from the emission spectra of PFP-NMe<sub>3</sub><sup>+</sup> in water–DMSO (19:1, v/v) mixture with various concentrations of **3**

[ <b>3</b> ] / $\mu\text{M}$	$K_{SV} \times 10^{-5} / \text{M}^{-1}$
0	–
5.0	2.3
10.0	2.6
15.0	3.5
20.0	5.2
25.0	8.9
30.0	15.0
35.0	89.8
40.0	263.2
45.0	435.6
50.0	426.0

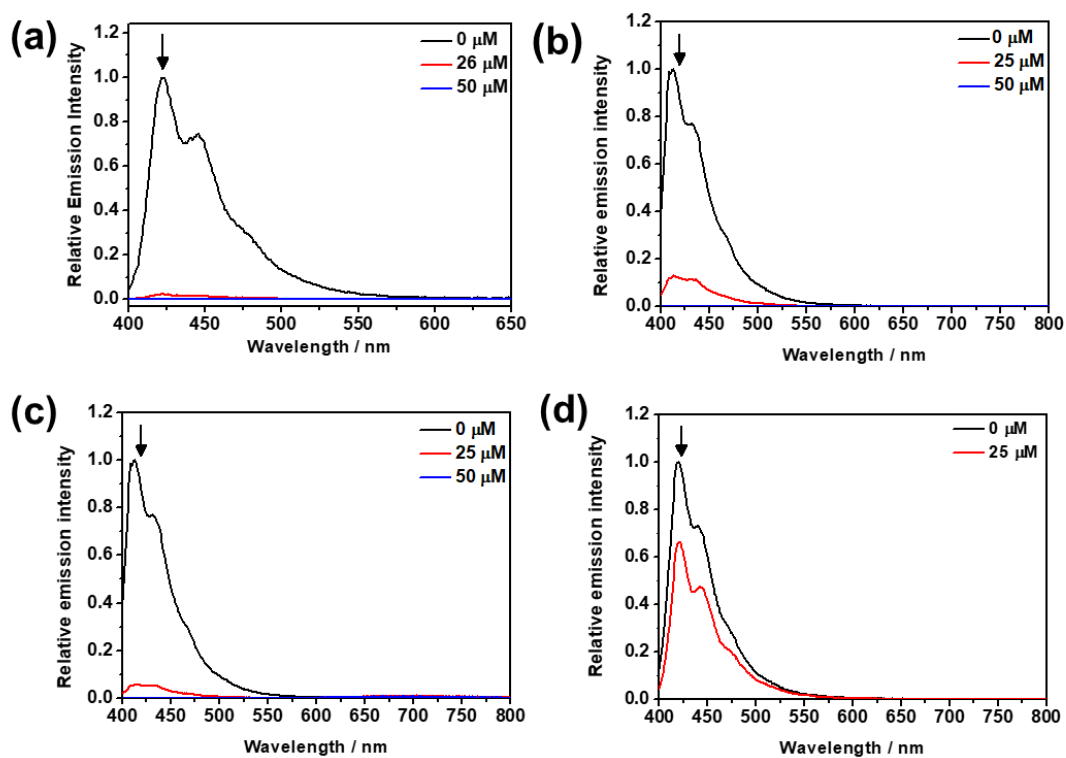


**Figure S7.** Emission spectral changes of PFP-NMe<sub>3</sub><sup>+</sup> (50 μM) upon addition of different concentrations of (a) **1** in water, (b) **2** and (c) **3** in water–DMSO (19:1, v/v) mixture as well as (d) **4** in water. Excitation wavelengths of 355 nm for **1** and **4** as well as 385 nm for **2** and **3** were used.

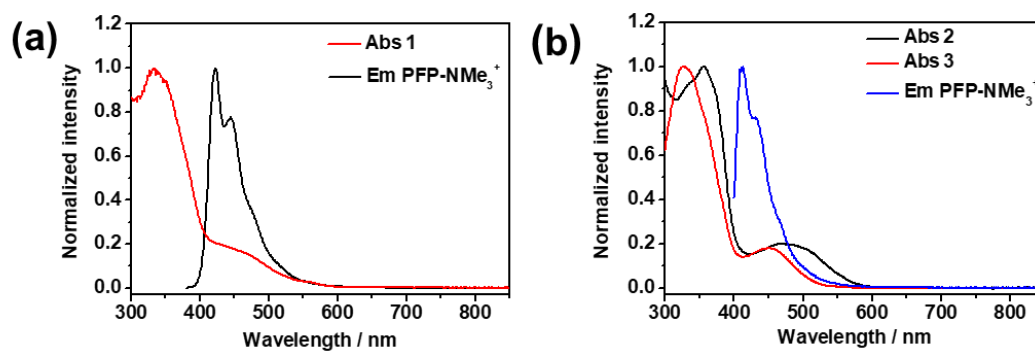


**Figure S8.** (a) Normalized electronic absorption spectrum of **1** (red) and the emission spectrum of PFP-NMe<sub>3</sub><sup>+</sup> (black) in water showing the spectral overlap. (b) Normalized electronic absorption spectra of **2** (black), **3** (red) and the emission spectrum of PFP-NMe<sub>3</sub><sup>+</sup> (blue) in water–DMSO (19:1, v/v) mixture showing the spectral overlap. The concentration of **1–3** and the trimethylammonium groups in PFP-NMe<sub>3</sub><sup>+</sup> are 50 μM. Excitation wavelengths of 355 nm in water and 385 nm in water–DMSO (19:1, v/v) mixture for PFP-NMe<sub>3</sub><sup>+</sup> were used.

**Table S5.** Parameters obtained from the equation determining the Förster radius,  $R_0$ ,<sup>a</sup> of **1–3**

Complex	Conjugated polymer	$\Phi_{\text{lum}}^{\text{d}}$	$J^{\text{e}} / \text{cm}^2 \text{nm}^4 \text{mol}^{-1}$	$R_0^{\text{f}} / \text{Å}$
<b>1</b>	PFP-NMe <sub>3</sub> <sup>+b</sup>	0.36	$5.6 \times 10^{15}$	58
<b>2</b>	PFP-NMe <sub>3</sub> <sup>+c</sup>	0.33	$6.6 \times 10^{15}$	59
<b>3</b>	PFP-NMe <sub>3</sub> <sup>+c</sup>	0.33	$6.8 \times 10^{15}$	59

<sup>a</sup> $R_0 = 0.211[\kappa^2 n^4 \Phi_{\text{D}} J(\lambda)]^{1/6}$ .

<sup>b</sup>Measured in water.

<sup>c</sup>Measured in water–DMSO (19:1, v/v).

<sup>d</sup>The relative luminescence quantum yield was measured at ambient temperature with reference to quinine sulfate in 1.0 N H<sub>2</sub>SO<sub>4</sub>.

<sup>e</sup>Donor–acceptor spectral integral overlap, where the absorption spectra of the aggregated platinum(II) complexes were recorded in the presence of non-conjugated poly(diallyldimethylammonium chloride) instead of PFP-NMe<sub>3</sub><sup>+</sup> to minimize the interference from absorption of the conjugated polymer.

<sup>f</sup>Förster radius of the platinum(II) complexes with PFP-NMe<sub>3</sub><sup>+</sup>.

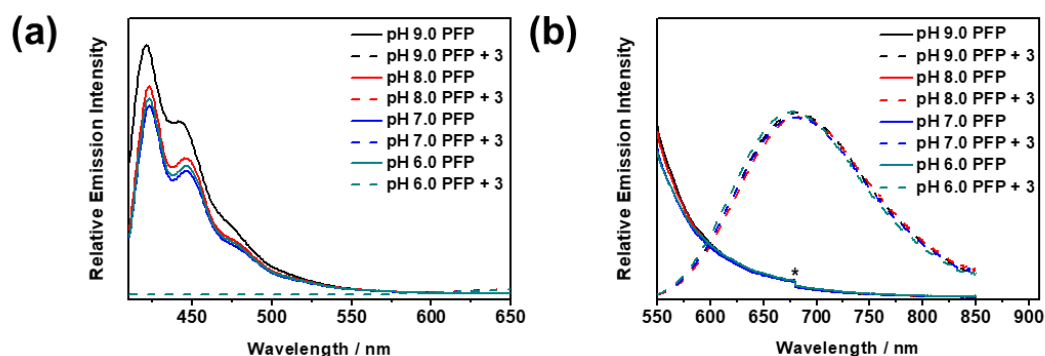


**Figure S9.** Emission spectral changes of PFP-NMe<sub>3</sub><sup>+</sup> (50 μM) in Tris-HCl buffer (5 mM, 5 % DMSO v/v, pH 6.0–9.0) upon addition of **3** (50 μM) in the range of (a) 410–650 nm and (b) 550–850 nm. An excitation wavelength of 385 nm was used.

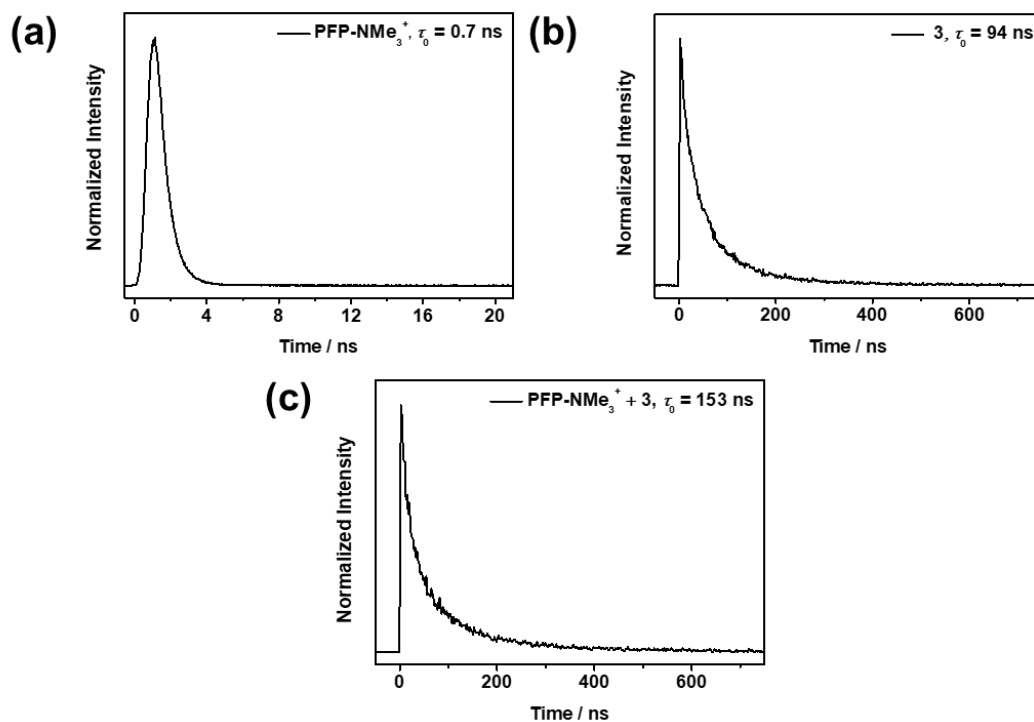


**Figure S10.** Time-resolved phosphorescence decay traces (detected at the emission band maxima) of (a) PFP-NMe<sub>3</sub><sup>+</sup> in the range of 0–21 ns, (b) **3** and (c) ensemble of **3** and PFP-NMe<sub>3</sub><sup>+</sup> in the range 0–750 ns. The measurements were performed in degassed water–DMSO (19:1, v/v) mixture at 298 K and the decay traces were fitted over a monoexponential model.

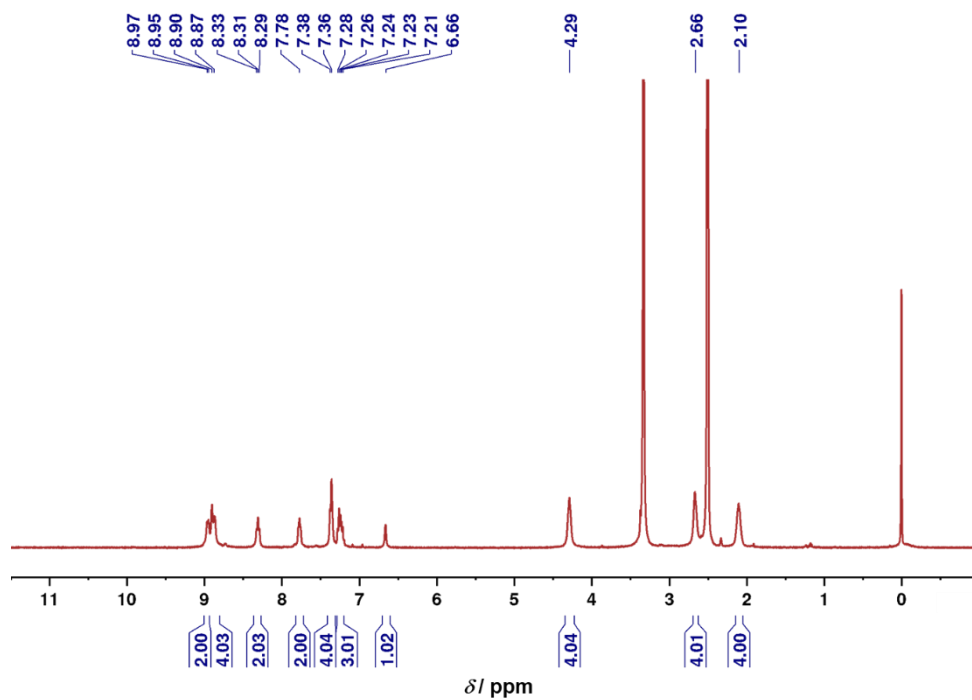


Figure S11.  $^1\text{H}$  NMR spectrum of **1** in  $\text{DMSO-}d_6$  at 298 K.

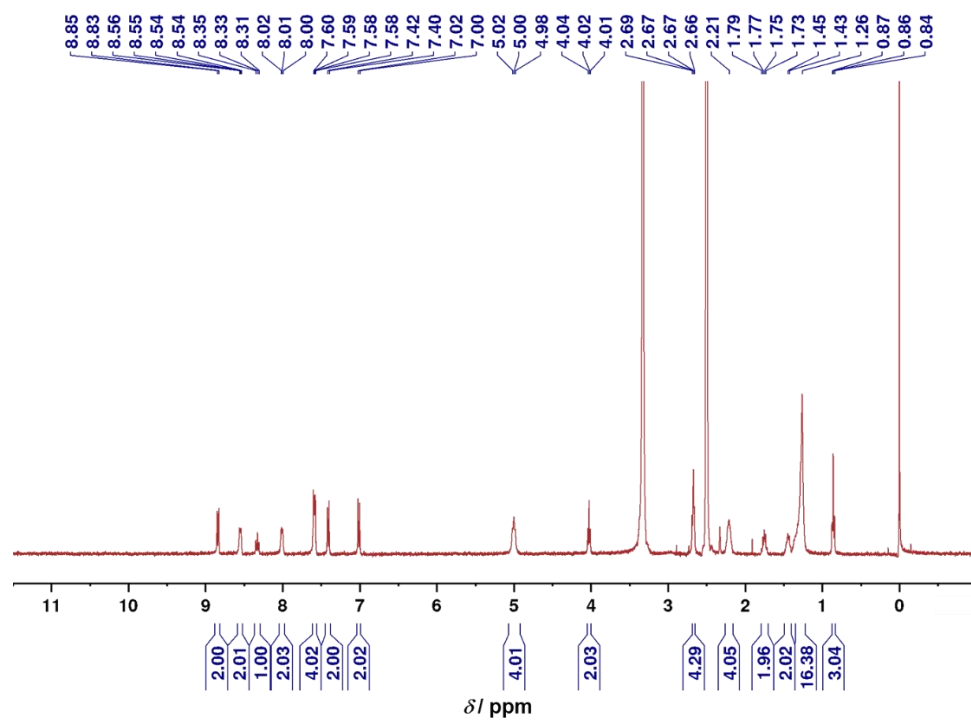


Figure S12.  $^1\text{H}$  NMR spectrum of **2** in  $\text{DMSO-}d_6$  at 298 K.

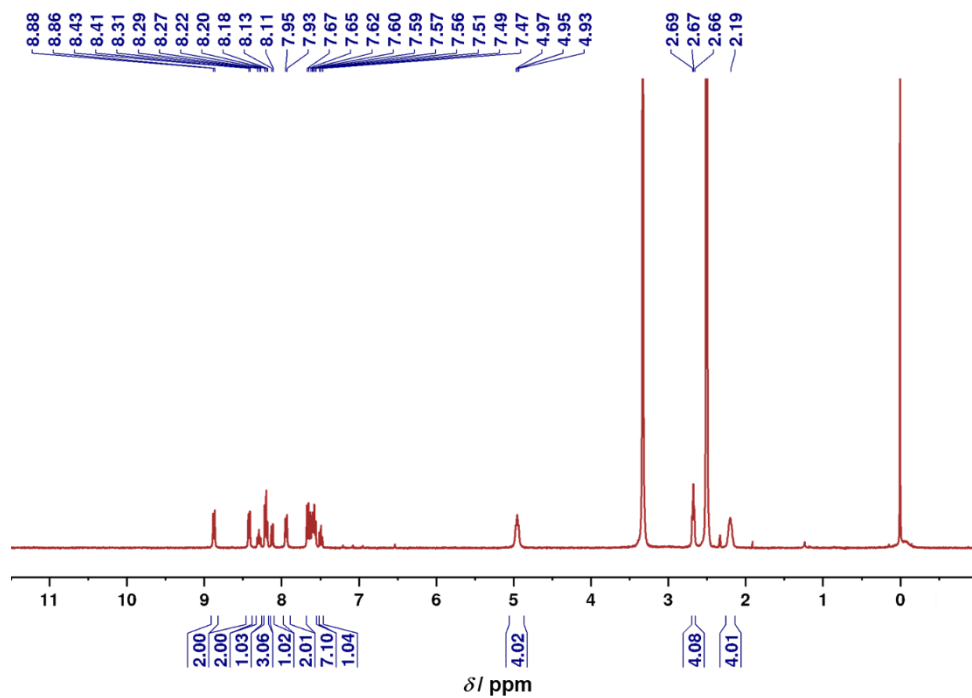


Figure S13.  $^1\text{H}$  NMR spectrum of **3** in  $\text{DMSO-}d_6$  at 298 K.

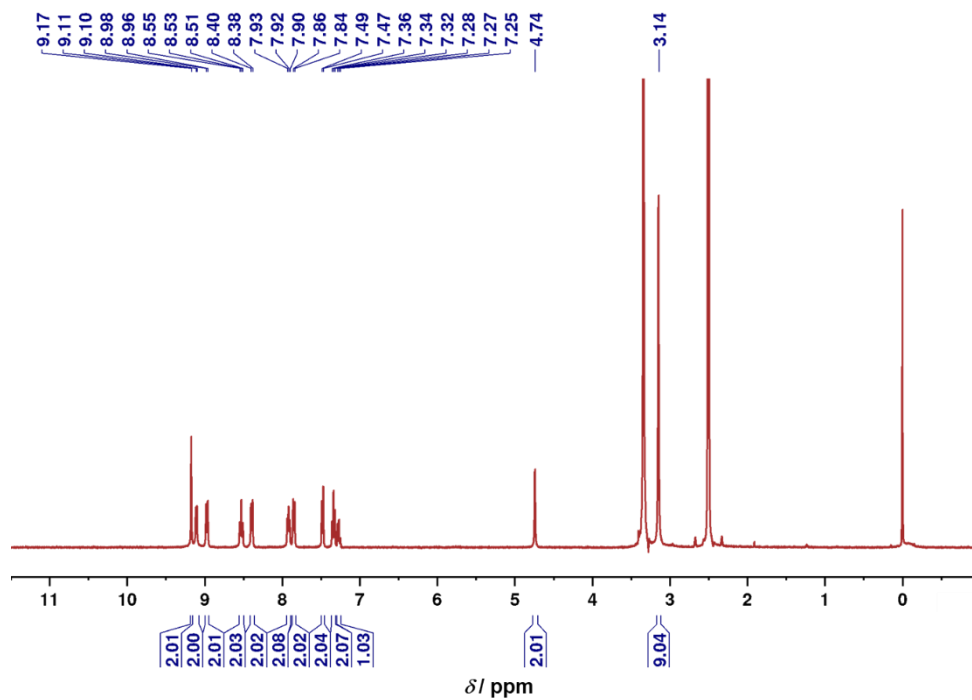


Figure S14.  $^1\text{H}$  NMR spectrum of **4** in  $\text{DMSO-}d_6$  at 298 K.

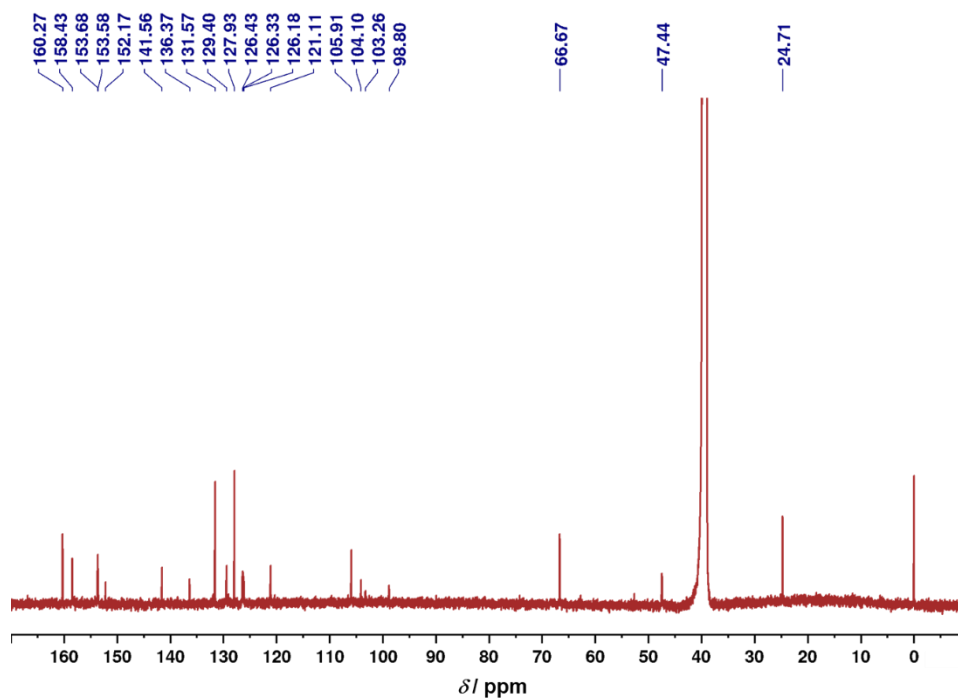


Figure S15.  $^{13}\text{C}\{^1\text{H}\}$  NMR spectrum of **1** in  $\text{DMSO-}d_6$  at 298 K.

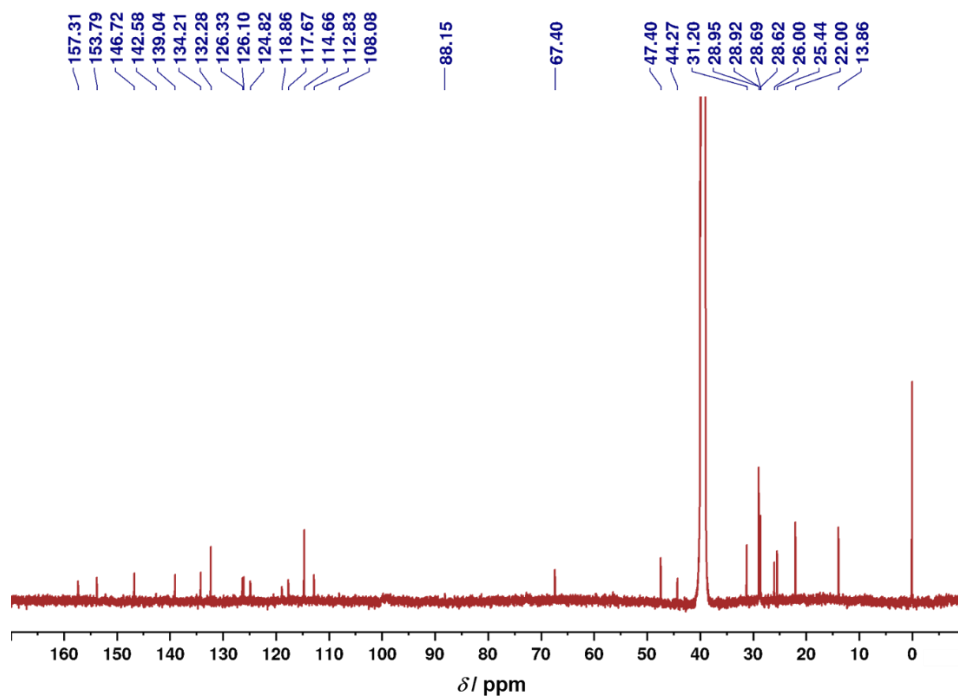
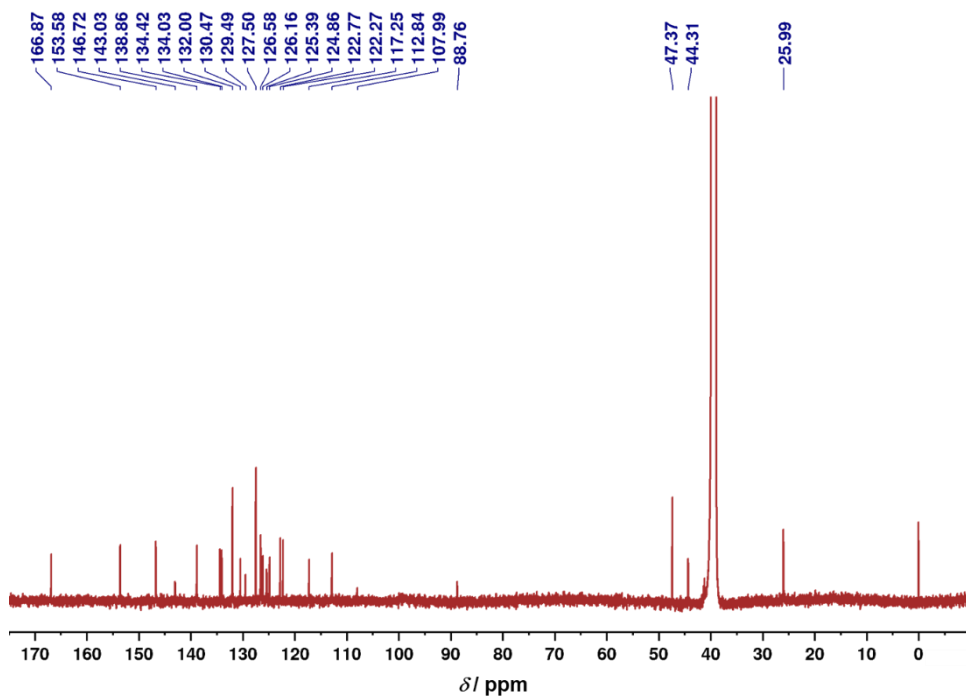
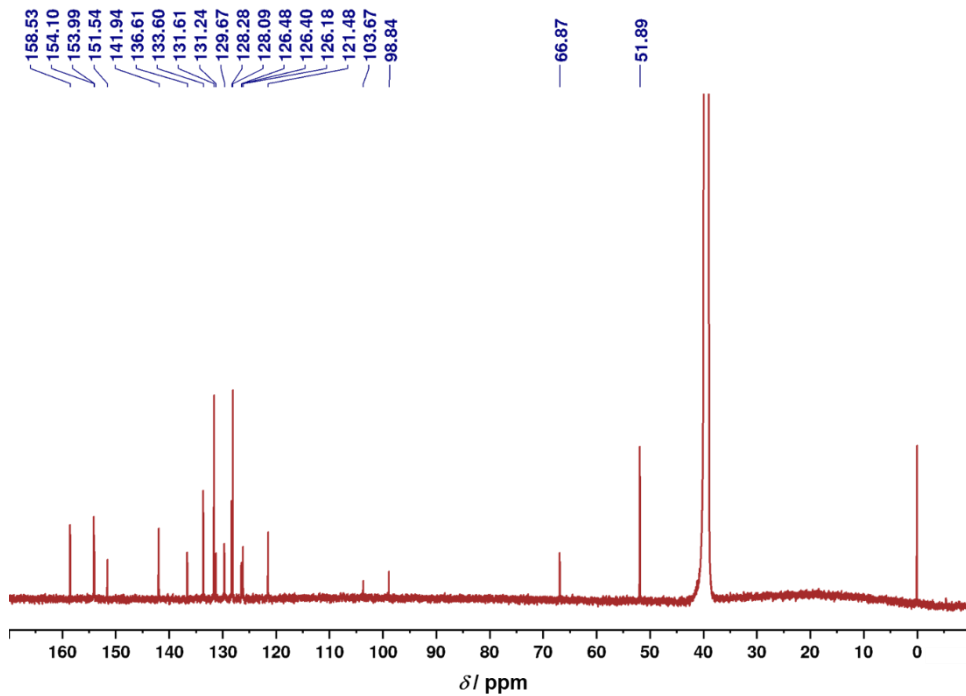


Figure S16.  $^{13}\text{C}\{^1\text{H}\}$  NMR spectrum of **2** in  $\text{DMSO-}d_6$  at 298 K.



**Figure S17.**  $^{13}\text{C}\{^1\text{H}\}$  NMR spectrum of **3** in  $\text{DMSO-}d_6$  at 298 K.



**Figure S18.**  $^{13}\text{C}\{^1\text{H}\}$  NMR spectrum of **4** in  $\text{DMSO-}d_6$  at 298 K.

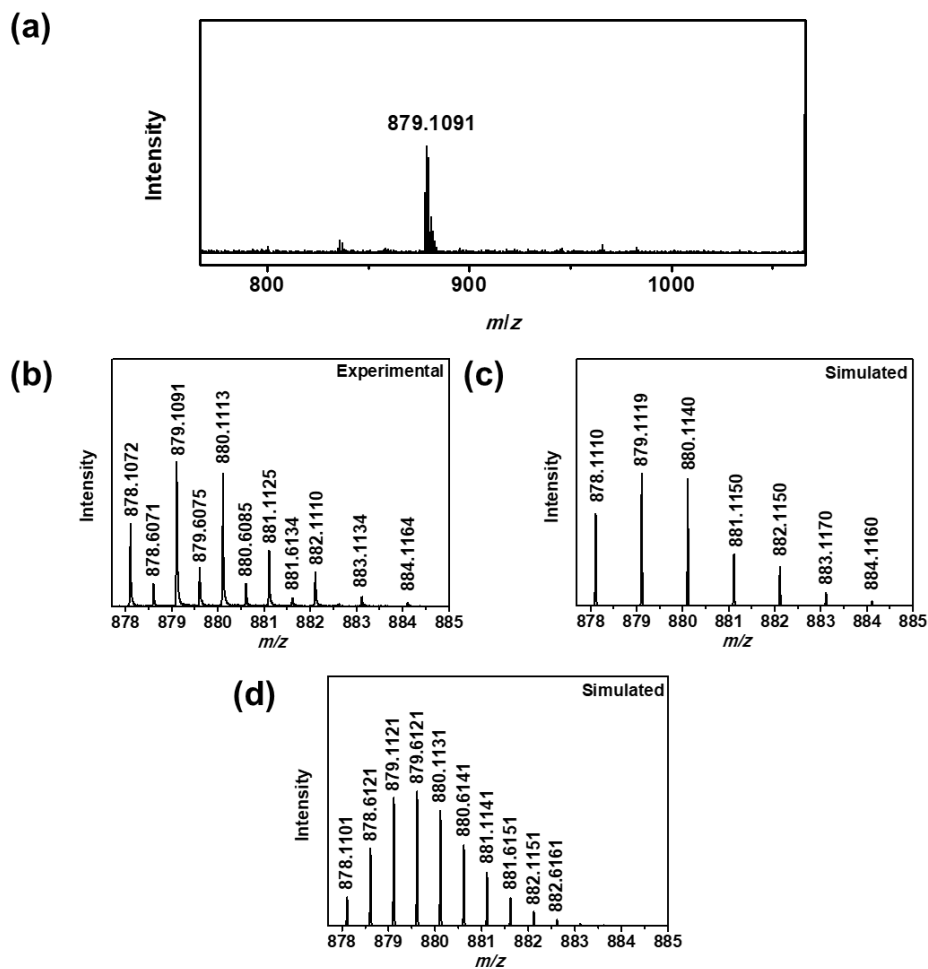


**Figure S19.** (a) Full high-resolution negative ESI mass spectrum of **1** and (b) expanded ion cluster at  $m/z$  879. Simulated isotopic patterns for (c)  $[M-K]^-$  and (d)  $[2M-2K]^{2-}$  ion clusters.

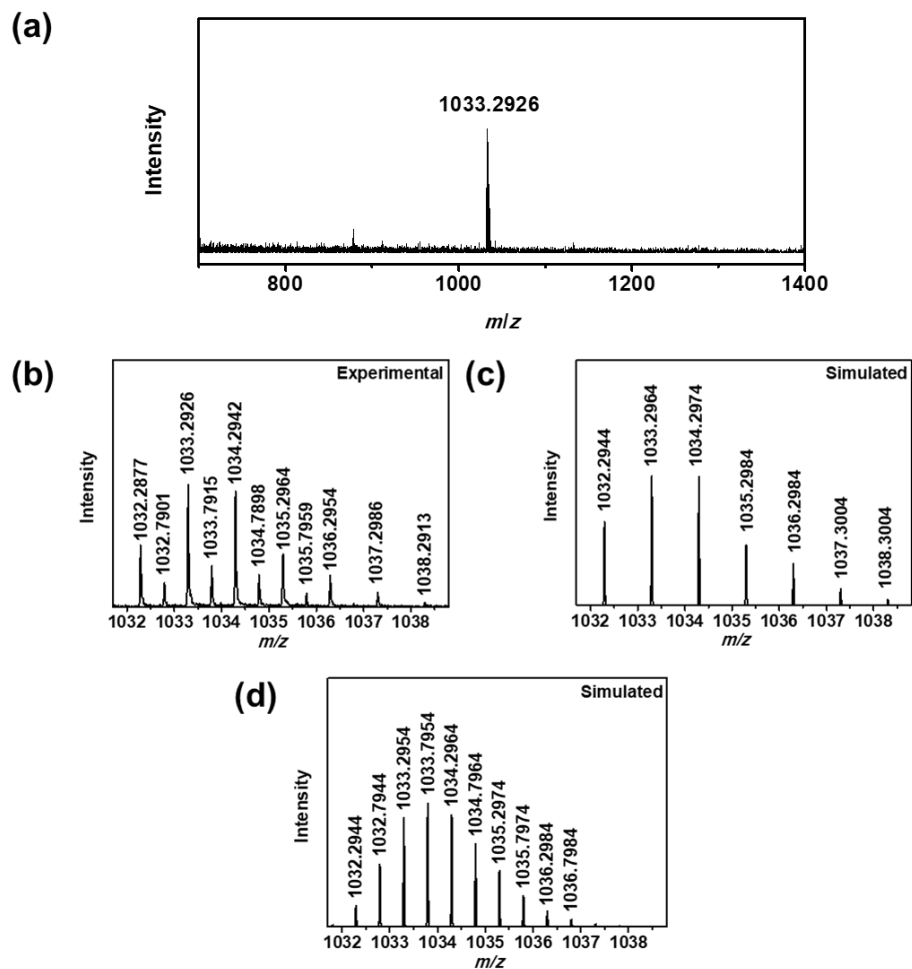


**Figure S20.** (a) Full high-resolution negative ESI mass spectrum of **2** and (b) expanded ion cluster at  $m/z$  1033. Simulated isotopic patterns for (c)  $[M-K]^-$  and (d)  $[2M-2K]^{2-}$  ion clusters.

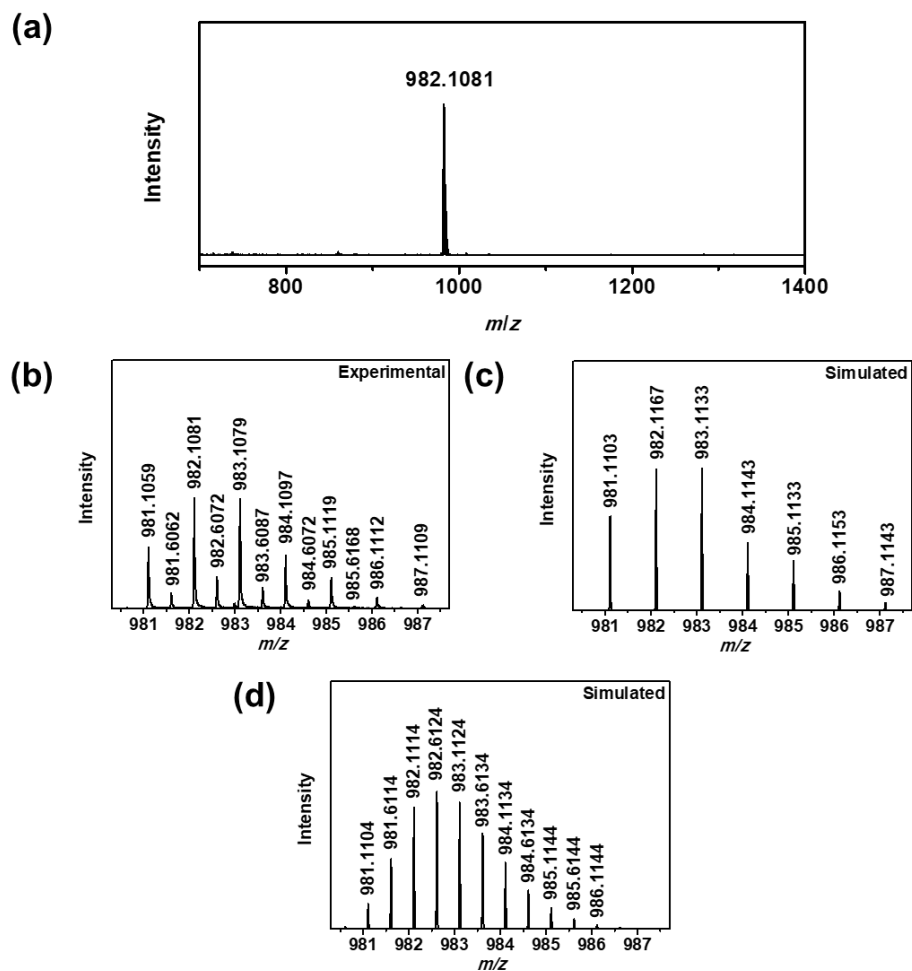


**Figure S21.** (a) Full high-resolution negative ESI mass spectrum of **3** and (b) expanded ion cluster at  $m/z$  982. Simulated isotopic patterns for (c)  $[M-K]^-$  and (d)  $[2M-2K]^{2-}$  ion clusters.

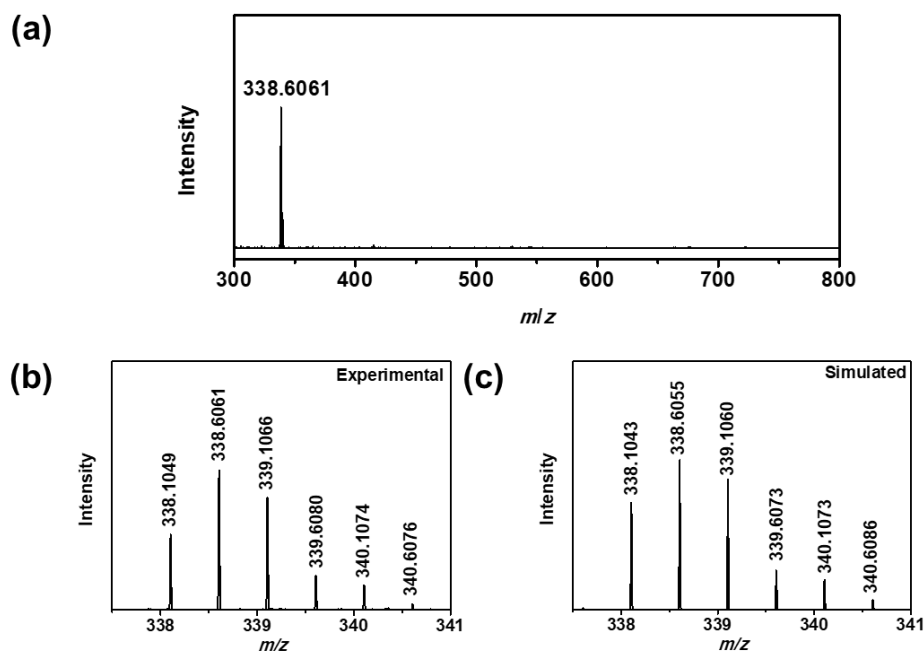


**Figure S22.** (a) Full high-resolution positive ESI mass spectrum of **4** and (b) expanded ion cluster at  $m/z$  339. (c) Simulated isotopic pattern for  $[M-2Cl]^{2+}$  ion cluster.

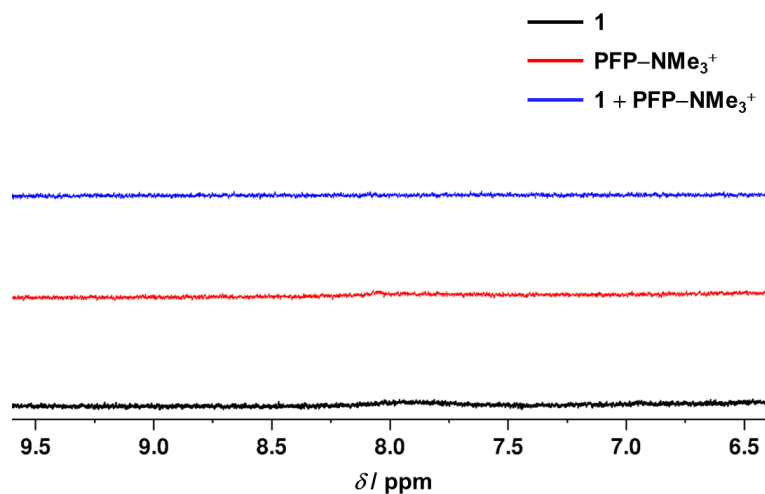


**Figure S23.** Partial  $^1H$  NMR spectra of **1** (black),  $PFP-NMe_3^+$  (red), as well as ensemble of **1** and  $PFP-NMe_3^+$  (blue) in  $D_2O$  in the aromatic region at 298 K.

## References

1. G. A. Crosby and J. N. Demas, Measurement of Photoluminescence Quantum Yields. Review, *J. Phys. Chem.*, 1971, **75**, 991-1024.
2. W. H. Melhuish, Quantum Efficiencies of Fluorescence of Organic Substances: Effect of Solvent and Concentration of the Fluorescent Solute, *J. Phys. Chem.*, 1961, **65**, 229-235.
3. B. Liu, S. Wang, G. C. Bazan and A. Mikhailovsky, Shape-Adaptable Water-Soluble Conjugated Polymers, *J. Am. Chem. Soc.*, 2003, **125**, 13306-13307.
4. Y.-S. Wong, F. C.-M. Leung, M. Ng, H.-K. Cheng and V. W.-W. Yam, Platinum(II)-Based Supramolecular Scaffold-Templated Side-by-Side Assembly of Gold Nanorods through Pt...Pt and  $\pi$ - $\pi$  Interactions, *Angew. Chem. Int. Ed.*, 2018, **57**, 15797-15801.
5. C. Po, A. Y.-Y. Tam, K. M.-C. Wong and V. W.-W. Yam, Supramolecular Self-Assembly of Amphiphilic Anionic Platinum(II) Complexes: A Correlation between Spectroscopic and Morphological Properties, *J. Am. Chem. Soc.*, 2011, **133**, 12136-12143.
6. C. Y.-S. Chung, S. P.-Y. Li, M.-W. Louie, K. K.-W. Lo and V. W.-W. Yam, Induced Self-Assembly and Disassembly of Water-Soluble Alkynylplatinum(II) Terpyridyl Complexes with "Switchable" Near-Infrared (NIR) Emission Modulated by Metal-Metal Interactions over Physiological pH: Demonstration of pH-Responsive NIR Luminescent Probes in Cell-Imaging Studies, *Chem. Sci.*, 2013, **4**, 2453-2462.
7. D. Thibeault, M. Auger and J.-F. Morin, Synthesis of Fluorine-Containing Molecular Rotors and Their Assembly on Gold Nanoparticles, *Eur. J. Org.*

- Chem.*, 2010, **2010**, 3049-3067.
8. J. E. Haley, D. M. Krein, J. L. Monahan, A. R. Burke, D. G. McLean, J. E. Slagle, A. Fratini and T. M. Cooper, Photophysical Properties of a Series of Electron-Donating and -Withdrawing Platinum Acetylide Two-Photon Chromophores, *J. Phys. Chem. A*, 2011, **115**, 265-273.
  9. C. Po, A. Y.-Y. Tam and V. W.-W. Yam, Tuning of Spectroscopic Properties *via* Variation of the Alkyl Chain Length: A Systematic Study of Molecular Structural Changes on Self-Assembly of Amphiphilic Sulfonate-Pendant Platinum(II) Bzimp Complexes in Aqueous Medium, *Chem. Sci.*, 2014, **5**, 2688-2695.
  10. X. T. Zheng, Y. C. Lai and Y. N. Tan, Nucleotide-Derived Theranostic Nanodots with Intrinsic Fluorescence and Singlet Oxygen Generation for Bioimaging and Photodynamic Therapy, *Nanoscale Adv.*, 2019, **1**, 2250-2257.
  11. H. Chen, S. Li, M. Wu, Kenry, Z. Huang, C.-S. Lee and B. Liu, Membrane-Anchoring Photosensitizer with Aggregation-Induced Emission Characteristics for Combating Multidrug-Resistant Bacteria, *Angew. Chem. Int. Ed.*, 2020, **59**, 632-636.